7
Ion Flux and Ligand Binding Assays for Analysis of Ion Channels

Georg C. Terstappen

7.1
Introduction

Ion channels are pore-forming membrane proteins which enable the rapid passage (flux) of ions across cell membranes. Their ion conductivity is often highly specific and has been used for their general classification into sodium, potassium, calcium, chloride and nonselective cation channels. As opposed to active transport by membrane pumps such as the Na^+/K^+ ATPase, ion channels allow only passive transport of ions along a concentration gradient. Their opening and closing ('gating') is regulated by a range of different stimuli including transmembrane voltage, ligand binding, mechanical stress and temperature. The first two stimuli are the most common and therefore these membrane proteins are broadly grouped into voltage-gated and ligand-gated ion channels.

Ion channels are central to many biological and disease processes and are particularly important for regulating electrical properties of excitable cells such as neurons and myocytes. In many other cell types they contribute to important physiological processes such as hormonal secretion and blood pressure regulation. Although ion channels constitute a complex gene family one common feature is a pore-forming region which determines ion selectivity and mediates ion flux across cell membranes. The recent sequencing of the human genome has revealed around 400 pore-forming ion channel genes corresponding to about 1.3% of the human genome [1]. These pore-forming ion channel subunits (α-subunits) contain a minimum of 2 trans-membrane domains, as in the case of the inward rectifying K^+ channel Kir, and up to 24 transmembrane domains, as in the case of voltage-gated Na^+ and Ca^{2+} channels. Some K^+ channels contain two pore-forming regions in tandem. Additional complexity is generated since functional ion channels are often homo- or heteromeric protein complexes which can co-assemble with accessory (β- and further) subunits, thus creating a vast number of physiological ion channel complexes with different functions and pharmacology. A significant number of disease relevant ion channels have been identified and in conjunction with novel assay technologies [2] and mechanistic insights into channel function the development of selective and state-dependent drugs is on the horizon.

Expression and Analysis of Recombinant Ion Channels. Edited by Jeffrey J. Clare and Derek J. Trezise

ISBN: 3-527-31209-9

7.2 Ion Flux Assays

Activation of ion channels leads to a movement of charged molecular species across the cell membrane. This ion flux along a concentration gradient leads to changes in membrane potential that can be quantified by the Nernst equation (Fig. 7.1). If ions that pass through the channel under study can be radiolabeled, radioactive flux assays can be developed for functional analysis and screening of these ion channels. If such ions are not available, or the use of radioactive isotopes needs to be avoided, ions that pass through the channel can also be analyzed by atomic absorption spectrometry, a technique traditionally used for the detection of trace elements in environmental, biological and medical samples. In any case, a cellular system is necessary that either natively or recombinantly expresses the ion channel of interest. Typically, mammalian cells such as HEK293 or CHO-K1 are employed for recombinant expression of ion channels although some channels need other cellular 'backgrounds' for proper functional expression [3] (see Chapter 4). Since functional ion flux assays represent a direct measure of channel activity, they are robust and insensitive to disturbances. Compared to electrophysiological methods which can be considered the 'gold standard' for functional analysis of ion channels, their temporal resolution is limited to the sec-

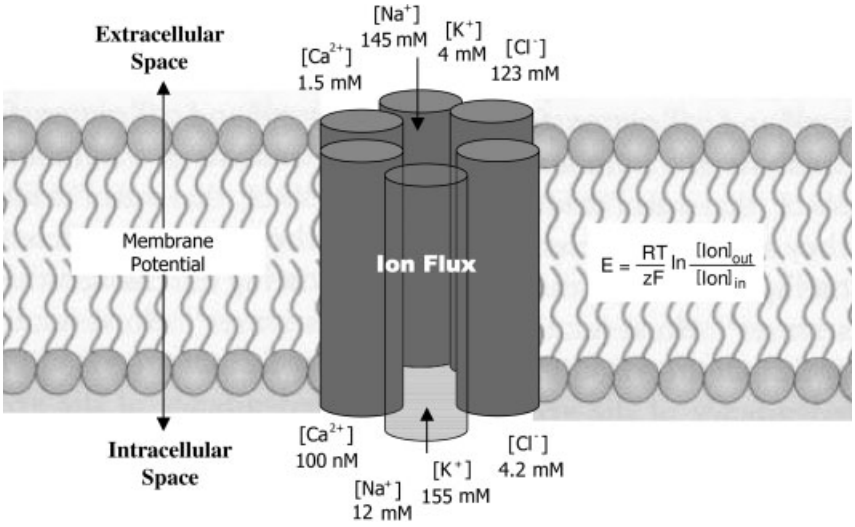

Fig. 7.1 In cellular systems activation of ion channels leads to ion flux along a concentration gradient and concomitant changes in transmembrane potential which can be quantified by the Nernst equation (shown on the right). If radioactively labeled ions are added or if K^+ or Na^+ ions are exchanged with Rb^+ or Li^+ (see text), changes in ion concentrations can be determined by measurement of radioactivity or atomic absorption spectrometry, respectively. Both measurements represent the basis for the development of functional assays to monitor ion channel activation. Shown free intra- and extracellular ion concentrations have been taken from Ref. [12].

onds/minutes range and the membrane potential cannot be controlled precisely. Thus, these assays cannot be employed for screening of *bona fide* state-dependent ion channel modulators.

7.2.1 Radioactive Ion Flux Assays

The application of radioactive isotopes of ions that pass through the channel under study – and thus can serve as tracers for these ions in cellular assay systems – has long been used.

Radioactive isotopes of the naturally conducting ion species, such as $^{22}Na^{+}$ [4], $^{45}Ca^{2+}$ [5] and $^{36}Cl^{-}$ [6], can be employed as tracers as can other radioactive ion species which are conducted by the channel. For instance, $^{86}Rb^{+}$ has been used for the study of potassium and nonselective cation channels [7] and ^{14}C-guanidinium for analysis of sodium channels [4]. Based on transmembrane concentration gradient and ion conductivity (Fig. 7.1) influx of radiotracer is usually measured for sodium, calcium and chloride channels, whereas efflux is measured for potassium channels upon activation. Cells expressing the ion channel of interest are typically grown in standard cell culture compatible microplates. Voltage-gated channels are activated by adding a 'depolarizing' concentration of ≥ 50 mM KCl to the cell medium whereas other channels are, for instance, activated by adding an appropriate concentration of ligand. Measurement of radioactivity using standard equipment is either carried out in the cell supernatant, the cell lysate or both matrices by direct Cerenkov counting (e.g. ^{86}Rb) or liquid scintillation counting (e.g. ^{45}Ca). Measurements of both matrices allow calculation of the relative flux of radiotracer thus eliminating potential well-to-well differences in cell densities and tracer loading.

A homogeneous radioactive ion flux assay format is possible using CytoStar-T scintillating technology (GE Healthcare) employing β-emitting isotopes. Based on the principles of scintillation proximity assay (SPA) technology (see Section 7.3) each well of a special microplate is coated at the bottom with scintillant that will only detect radioisotopes in close vicinity to it. Thus, if cells are cultured as monolayers on these plates and channels are activated in the presence of radiotracer, the influx or efflux can be measured as a change of light using any plate-based scintillation counter. With this technique, no wash steps and no separation of initially applied radiotracer are necessary thus making this assay format more amenable to the requirements of high throughput screening (HTS). A few examples of measuring influx of ^{14}C-guanidinium for sodium channels [8], influx of $^{45}Ca^{2+}$ for ionotropic glutamate receptors [9] and efflux of $^{86}Rb^{+}$ for potassium channels [10] have been described.

A major advantage of radioactive ion flux assays is that no special apparatus is necessary if the laboratory is equipped for the measurement of radioactivity, which is usually the case in both academic and industrial environments. The main disadvantage of flux assays is the use of radioisotopes which is associated with significant costs, safety hazards and environmental (e.g. disposal) problems. This is the

main reason why radioactive ion flux assays, which were frequently used in the 1990s in the pharmaceutical industry, have largely been abandoned and replaced by nonradioactive alternatives such as nonradioactive ion flux assays based on atomic absorption spectrometry (Section 7.2.2) and fluorescence-based assays (see Chapter 8).

7.2.2
Nonradioactive Ion Flux Assays based on Atomic Absorption Spectrometry

Atomic absorption spectrometry (AAS) is a well established technology, traditionally used for the detection of trace elements in environmental, biological and medical samples, that uses thermal energy to generate free ground state atoms in a vapor phase which absorb light of a specific wavelength. In practice, atomization is achieved by spraying a sample containing the element to be measured into the flame of the burner of an atomic absorption spectrometer. Absorption of light, which is typically emitted by hollow cathode lamps, is measured with a photomultiplier (Fig. 7.2). Thus, an atomic absorption spectrometer can be imagined as a photometer where the *cuvette* is replaced by a burner generating the flame ("flame photometry"). The law of *Lambert–Beer–Bouger* applies and can be employed to determine the concentration of an element by measuring its absorption. In practice, however, this is usually done by comparing the light absorption of a sample with a standard curve obtained under identical experimental conditions.

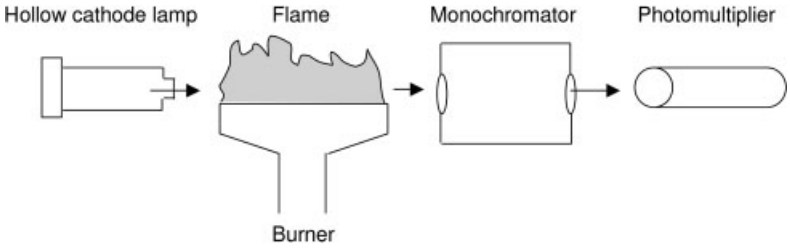

Fig. 7.2 Schematic diagram of an atomic absorption spectrometer. For details refer to the text.

7.2.2.1 Nonradioactive Rubidium Efflux Assay

An AAS-based rubidium efflux assay for functional analysis of potassium and nonselective cation channels was established in the 1990s [11]. Rubidium is an alkali metal with atomic number 37 and an ionic radius of 1.61 Å which is not present in eukaryotic cells. Its similarity to K^+ leads to a high permeability in potassium and nonselective cation channels [12]. It can easily be detected by using atomic absorption spectrometry with a sensitivity ('characteristic concentration') of 0.11 mg l^{-1} measuring absorption at 780 nm.

In general, the experimental protocol for a nonradioactive Rb^+ efflux assay consists of two parts, cell biology and physical determination of the tracer rubidium by AAS. First, cells expressing the ion channel under study are cultured in cell compatible microplates and loaded with rubidium by simply exchanging potassium in a cell compatible buffer solution with the same concentration of rubidium. This loading phase, which is usually finished within 2–4 h, can be inhibited by the cardiac glycoside oubain, pointing to the involvement of Na^+/K^+-ATPases in transporting Rb^+ into the cells. Prior to starting efflux experiments it is necessary to remove excess Rb^+ by a series of quick wash steps with buffer containing KCl. The frequency and buffer volumes used for these wash steps mainly depend on the cell type, cell density, microplate formats and washing devices employed and should be optimized on a *case-by-case* basis since appropriate removal of excessive Rb^+ is essential in order to obtain good signal-to-background ratios. Activation of the ion channel under study leads to Rb^+ efflux into the cell supernatant due to the established concentration gradient for this tracer ion (see also Fig. 7.1). For voltage-gated potassium channels activation can be achieved by adding a depolarizing concentration of KCl (typically ≥ 50 mM) to the cells and for ligand-gated channels by adding an appropriate concentration of ligand. The incubation time with the channel activator has to be optimized empirically in order to achieve optimal efflux results but in most cases a period of ≥ 10 min is sufficient. When compounds are screened for channel blocking effects they should be added prior to channel activation (e.g. 10 min) because of kinetic considerations. Cell supernatants which contain the 'effluxed' Rb^+ are removed and collected along with the cell lysates. Both of these Rb^+-containing matrices can be stored at room temperature prior to AAS analysis which is not disturbed by cell debris.

In principle, rubidium determinations can be carried out with any type of flame atomic absorption spectrometer and measurements should be carried out according to the instructions of the manufacturer. The recent development of an innovative AAS instrument for ion channel analysis (ICR 12000, Aurora Biomed Inc., Vancouver, Canada), featuring a sophisticated microsampling process utilizing 96- or 384-well microplates and simultaneous measurements of 12 samples at a time, allows the measurement of up to 60 000 samples per day (http://www.aurorabiomed.com/ICR12000.htm), making the nonradioactive Rb^+ efflux assay compatible with the throughput requirements of HTS in drug discovery.

Typically, the relative amount of rubidium in the supernatant is calculated as [Rb in supernatant/Rb in supernatant + Rb in cell lysate] thus eliminating potential well-to-well differences in cell densities and Rb^+ loading. This relative rubidium efflux is a robust and direct measure of ion channel activity and a $\geq$twofold increase of Rb^+ efflux upon channel activation over basal efflux levels is usually sufficient for the configuration of good quality HTS assays [13] since the standard deviations for rubidium measurements by AAS are low [11]. If sample throughput needs to be increased, under highly standardized experimental conditions it might be possible to measure rubidium only in the supernatant.

The following assay protocol for the analysis of calcium-activated BK_{Ca} channels [14] stably expressed in mammalian CHO-K1 cells was successfully used for func-

tional selection of stable recombinant clones expressing this ion channel and subsequent screening for the identification of channel modulators. This protocol can serve as a basis for the development of such assays for other potassium and nonselective cation channels.

Cells are grown at 37 °C in 96-well cell culture compatible microplates for 48 h to a final cell density of about 1×10^4 cells per well in standard cell culture medium. After aspirating the medium, 0.2 ml cell buffer containing RbCl is added (5.4 mM RbCl, 150 mM NaCl, 2 mM $CaCl_2$, 0.8 mM NaH_2PO_4, 1 mM $MgCl_2$, 5 mM glucose, 25 mM HEPES, pH 7.4) and cells are incubated for 4 h at 37 °C. Cells are then quickly washed three times with buffer (same as above, but containing 5.4 mM KCl instead of RbCl) to remove extracellular Rb^+. Subsequently, 0.2 ml buffer containing a saturating concentration of 25 µM of the Ca^{2+} specific ionophore A23187 (Fig. 7.3) is added to the cells in order to activate BK_{Ca} channels via a 'molecular Ca^{2+} injection' and after incubation for 10 min the supernatant is carefully removed and collected for rubidium measurements. Cells are lysed by the addition of 0.2 ml 1% Triton X-100 and also collected for rubidium determinations. AAS measurements are carried out with a flame atomic absorption spectrometer following the instructions of the manufacturer. The stimulated relative Rb^+ efflux [Rb in supernatant/Rb in supernatant + Rb in cell lysate] with these recombinant cells amounts to 80% (Fig. 7.4), which represents a five-fold increase over basal conditions. The specificity of the induced Rb^+ efflux is further demonstrated by the use of the specific BK_{Ca} channel ligand iberiotoxin isolated from the scorpion *Buthus tamulus* [15] which blocks the channel in a concentration-dependent manner with an IC_{50} of 15 nM (Fig. 7.5). If this protocol is used for the analysis of other potassium or nonselective cation channels, channel activation and specificity analysis have to be adapted appropriately.

In addition to the above mentioned example, a screening assay was developed for blockers of BK_{Ca} channels (Table 7.1) recombinantly expressed in HEK293 cells [16]. The diphenylurea analogue NS1608 was used to activate the channels

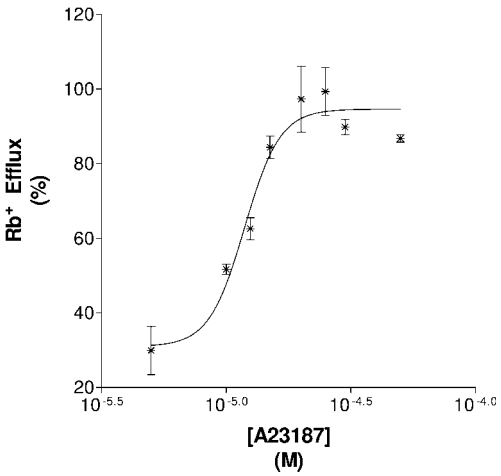

Fig. 7.3 Activation of BK_{Ca} channels recombinantly expressed in CHO-K1 cells with increasing concentrations of the calcium-specific ionophore A23187 leads to increasing Rb^+ efflux. For details refer to the text.

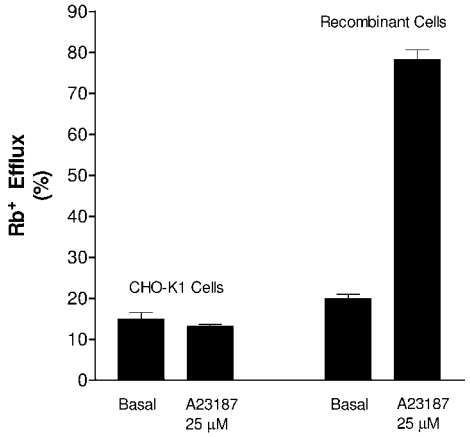

Fig. 7.4 The Rb^+ efflux induced with 25 µM of the ionophore A23187 is not observed in CHO-K1 cells which were used to generate the recombinant BK_{Ca} channel expressing cell line. For details refer to the text.

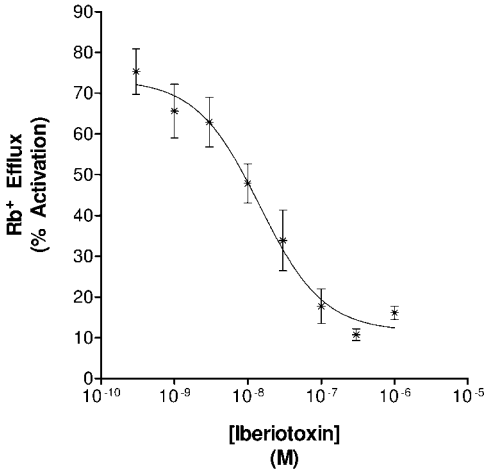

Fig. 7.5 Rb^+ efflux induced with 25 µM of the ionophore A23187 in recombinant CHO-K1 cells expressing BK_{Ca} channels is inhibited in a concentration-dependent manner with the selective ligand iberiotoxin. For details refer to the text.

leading to a three- to four-fold Rb^+ efflux which was completely blocked by the specific ligand iberiotoxin (IC_{50} = 12 nM). A pharmacological profile obtained with a series of known openers and blockers of BK channels compared very well with results obtained with a radioactive ^{86}Rb efflux assay [16], demonstrating the utility of the nonradioactive Rb^+ efflux assay for high throughput screening campaigns as well as SAR studies.

SK3 channels (Table 7.1) are one of three members of small conductance calcium-activated potassium (SK_{Ca}) channels [17] which are all activated by submicromolar increases in intracellular Ca^{2+} concentration mediated by calmodulin [18]. SK3 channels were recombinantly expressed in HEK293 cells [19] and the above described assay protocol was employed, activating channels by increasing intracellular Ca^{2+} concentrations with thapsigargin, an inhibitor of endoplasmatic Ca-ATPase which leads to a release of Ca^{2+} from intracellular stores (Fig. 7.6). Calcium activation of SK3 channels led to a two- to three-fold Rb^+ efflux which could

Table 7.1 Published examples of recombinant ion channels that have been analyzed employing nonradioactive Rb^+ efflux assay technology.

Voltage-gated K^+ channels	Ca^{2+}-activated K^+ channels	Ligand-gated nonselective cation channels
Kv1.1	SK_{Ca} (SK3)	Nondisclosed nonselective cation channel
Kv1.3	BK_{Ca}	
Kv1.4		
Kv1.5		
Kv7.2 (KCNQ2)		
Kv7.2/3 (KCNQ 2/3)		
Kv11 (hERG)		

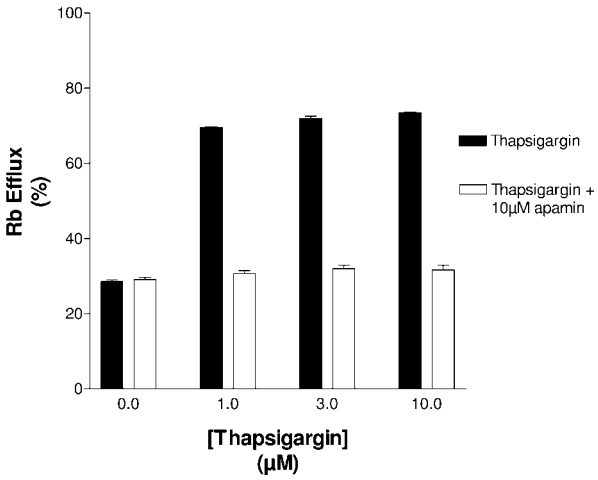

Fig. 7.6 Recombinant HEK293 cells expressing SK3 channels are activated by thapsigargin, an inhibitor of endoplasmatic Ca-ATPase which leads to release of Ca^{2+} from intracellular stores. Rb^+ efflux as measure of channel activity is completely blocked by the SK channel selective ligand apamin. For details refer to the text.

be completely blocked with the specific SK channel ligand apamin, a peptide present in bee venom toxin.

Nonradioactive Rb^+ efflux assays were developed for several recombinantly expressed voltage-gated potassium channels (Table 7.1). In the case of Kv1.1 and Kv1.4 channels expressed in HEK293 cells, activation with 50 mM KCl led to a less than twofold Rb^+ efflux in 10 min, which was blocked by the nonspecific potassium channel blocker TEA [11]. The relatively low KCl-induced Rb^+ efflux which was attributed to low expression levels and/or inactivation properties of the

channels was not sufficient to configure a robust screening assay. More recently, an assay was described for Kv1.3 channels expressed in CHO-K1 cells (http://www.aurorabiomed.com/New-Pro/CHO_Kv13_CellLine.pdf). Depolarization with 63 mM KCl led to a fourfold Rb^+ efflux in 15 min which could be blocked with an IC_{50} value of 0.66 nM by Agitoxin-2, a peptide blocker isolated from the venom of the scorpion *Leiurus quinquestriatus*. Although no further details were disclosed, the generation of a Kv1.5 expressing cell line for the establishment of a Rb^+ efflux assay was noted by Merck Research Laboratories at an ion channel conference in 2004 (http://www.aurorabiomed.com/retreat2004.htm). For Kv7.2 (KCNQ2) channels stably expressed in HEK293 cells stimulation with 50 mM KCl led to a fourfold Rb^+ efflux [20]. Calculated *Z'* factors [13] were 0.73 for a 96-well plate format and 0.6 for a 384-well format, respectively, indicating the high suitability for screening and SAR studies. The pharmacological profile of Kv7.2 defined by electrophysiology was faithfully reflected by the Rb^+ efflux assay which allowed measuring 1000 data points per day in a 96-well plate format [20]. For the identification of heteromeric Kv7.2/3 (KCNQ2/3) channel (M-current) modulators a recombinant CHO-K1 cell line expressing these channels was employed [21]. Channels were activated with 20 mM KCl in the presence of the channel opener Way-1 and an average *Z'* value of 0.81 for the 96-well format was calculated from a total of 20 experiments. A throughput of about 40 compounds per day for obtaining EC_{50} values (8-point curves) was achieved if AAS determinations of rubidium were only carried out in cell supernatants which gave results consistent with calculating relative Rb^+ efflux by measuring rubidium contents in both supernatants and cell lysates. Specificity was demonstrated by using the known M-current blocker linopirdine which inhibited Rb^+ efflux with an IC_{50} of 2.85 μM, a value in close agreement with results obtained from electrophysiological analysis.

The voltage-gated potassium channel Kv11 (hERG) seems to be particularly susceptible to inhibition by many xenobiotics and drugs leading to potentially lethal arrhythmias [22]. In fact, several drugs have recently been withdrawn from the market due to hERG channel activity. Thus, in drug discovery hERG channel liability of novel compounds is a major concern. A nonradioactive Rb^+ efflux assay was developed using hERG channels stably expressed in CHO-K1 cells [23]. Channels were activated by addition of 50 mM KCl for 10 min which resulted in an about two-fold Rb^+ efflux. Although the signal-to-background ratio was relatively low, a *Z'* value of 0.53 was calculated for a 96-well plate format thus meeting HTS standards. A pharmacological characterization employing a series of known hERG channel blockers (dofetilide, terfenadine, sertindole, astemizole, cisapride) showed the same rank order of potency as electrophysiology. Absolute IC_{50} values were 5–20-fold higher when compared to electrophysiological results obtained with mammalian cells but were similar to data in *Xenopus* oocytes. These results indicate the suitability of the Rb^+ efflux assay for hERG compound profiling. A similar recombinant cell line was also employed by AstraZeneca who disclosed results at an ion channel conference in 2003 (http://www.aurorabiomed.com/main-1.htm). In this case, a four-fold Rb^+ efflux was measured in a 384-well plate format after 30 min incubation with 50 mM KCl. The calculated *Z'* value was

≥0.5 utilizing the ICR 12000 atomic absorption spectrometer (Aurora Biomed, Vancouver, Canada).

Studies on native ligand-gated nonselective cation channels (nicotinic acetyl choline receptors and purinergic P2X receptors) in PC12 cells have also been described [11]. The development and application of nonradioactive Rb^+ efflux assays for such recombinantly expressed ion channels has, however, yet to be fully described. In a recent presentation from Amgen at an ion channel conference in 2003 a Rb^+ efflux assay for a non-disclosed ligand-gated cation channel expressed in CHO-K1 cells was overviewed (http://www.aurorabiomed.com/main-1.htm). Exposing the recombinant cells to 3–10 μM of a nondisclosed agonist resulted in an about four-fold Rb^+ efflux. This efflux was blocked by a nondisclosed antagonist with an IC_{50} of 344 nM which was in very good agreement with electrophysiological results, again demonstrating the reliability of such functional ion flux assays.

7.2.2.2 **Nonradioactive Lithium Influx Assay**

Due to the high sensitivity of AAS for the determination of Li^+ ions (0.035 mg l^{-1}), influx experiments for screening of sodium channels which display a high conductivity for Li^+ [12] should also be possible. Although no data have been published yet in scientific journals, at an ion channel conference in 2003 promising results obtained with SH-SY5Y cells were presented by AstraZeneca (www.aurorabiomed.-com/main-1.htm). Cells were differentiated for 3–5 days with retinoic acid which induces the expression of tetrodotoxin-sensitive voltage-gated sodium channels. Cells were washed with buffer in which NaCl was replaced with choline chloride in order to remove free Na^+. After incubation for 10 min at 37 °C in wash buffer, cells were treated with 5.4 mM KCl (basal) or 120 mM KCl (depolarization) in buffer containing LiCl for 15 min. After three wash steps at room temperature, cells were lysed with 1% Triton X-100 and cell lysates analyzed for Li^+ concentrations with AAS. Under these conditions, a three-fold Li^+ influx over basal levels was obtained which could be completely blocked by preincubation for 5 min with 1 μM tetrodotoxin. Results obtained with recombinantly expressed sodium channels are awaited.

7.2.2.3 **Nonradioactive Chloride Influx Assay**

A more indirect application of AAS-based methods for analysis of ion channels was briefly noted for the investigation of chloride channels [24]. In this case, Cl^- flux is measured after precipitating these ions with silver nitrate as AgCl and determining free silver by AAS. The utility of this indirect method remains to be established.

7.2.2.4 **Conclusions**

Taken together, nonradioactive ion flux assays based on AAS have largely displaced radioactive flux assays in drug discovery [25]. These assays represent a direct measure of channel activity, are HTS compatible if special equipment is used

and do not require radioactive isotopes. To date, their application has mainly been limited to the functional analysis and screening of potassium and nonselective cation channels. As compared to the 'gold standard' electrophysiology their temporal resolution is relatively low (seconds–minutes) and the transmembrane potential cannot be controlled precisely. Compared to other screening technologies such as fluorescence-based methods, these robust assays are less prone to identifying 'false positive' hits in drug screening programs and are thus highly reliable.

7.3 Ligand Binding Assays

Binding assays employing radiolabeled ligands have a long tradition in the study of receptors. For the investigation of ion channels, in particular for drug screening purposes, these assays were frequently used in the 1980s/1990s before more information-rich functional cell-based assays became available. The use of radiolabeled neurotoxins has revealed the existence of multiple binding sites for sodium channels [26] whereas the use of radiolabeled glibenclamide has been instrumental for the discovery of first and second generation sulfonylurea compounds (blockers of K_{ATP} channels) for treatment of type-2 diabetes [27]. More recently, radioligand binding assays have also been employed to investigate a potential hERG (Kv11) channel activity of novel compounds (see above) which might lead to potentially lethal arrhythmias [22]. The known hERG channel blockers dofetilide and MK-499 were used in tritiated form and as a ^{35}S analogue, respectively, to identify a hERG liability of compounds [28].

For the configuration of radioligand binding assays a radiolabeled ligand binding to the ion channel under study is necessary. Table 7.2 summarizes major ion channel radioligands that have been described to date. Furthermore, a source of the channel is also needed which can be organs, tissues or cells. Although binding assays can be performed with living cells cultured in microplates [3], usually cell membranes are prepared and utilized since they can be stored at –80 °C and are much easier to handle. In saturation experiments the affinity (K_d) of a radioactive ligand for the ion channel is determined whereas in competition (displacement) experiments the affinity of unlabeled ligands (K_i) is measured [29]. For screening purposes, which aim at the identification of novel chemical entities acting on ion channels, displacement experiments are carried out which can identify compounds that bind to the same site as the radioligand or sites allosterically coupled to it. Thus, such assays do not provide *bona fide* information about the effects of compounds on channel function. Usually the concentration of a compound necessary to displace 50 % of the radioligand (IC_{50} value) is determined as a measure of the compound's affinity for the channel. If K_i values are necessary, these can be calculated from IC_{50} values by using the Cheng–Prusoff equation [30]. Despite their ease and compatibility with the requirements of HTS, such ligand binding assays suffer from the need for radioisotopes such as ^{3}H and ^{125}I and the associated costs, safety hazards and environmental (e. g. disposal) problems.

Table 7.2 Major ion channel radioligands.

Channel	Type /Current	Radioligand	Ref.
calcium			
Ca_v 1	L	[^{3}H]-isradipine [^{3}H]-devapamil [^{3}H]-diltiazem [^{3}H]-DTZ323	37–39
Ca_v 2	P/Q N	[^{125}I]-ω-conotoxin GVIA [^{125}I]-ω-conotoxin MVIIC	40–42
sodium			
Na_v		[^{3}H]-saxitoxin [^{3}H]-batrachotoxin [^{125}I]-scorpion toxins [^{3}H]-tetrodotoxin [^{3}H]-brevetoxin [^{3}H]-PbTx-3	43–49
potassium			
Kv 1	Shaker-related	[^{125}I]-DT [^{125}I]-BgK [^{125}I]-DTX [^{125}I]-HgTX1 [^{125}I]-MgTx	50, 51
Kv 11	erg	[^{3}H]-astemizole [^{3}H]-dofetilide	52, 53
Kir 6	ATP-sensitive potassium channel	[^{3}H]-glibenclamide [^{125}I]-glibenclamide [^{125}I]-A312110 [^{3}H]-PKF217–744	54, 55
KCa 1	BK	[^{125}I]-charybdotoxin [^{125}I]-iberiotoxin [^{19}F]-BMS204352	56–58
KCa2	SK	[^{125}I]-apamin	59
nicotinic AChR		[^{3}H]-nicotine [^{3}H]-epibatidine [^{3}H]-cytisine [^{3}H]-MLA [^{3}H]-bungarotoxin [^{3}H]-tetracaine [^{3}H]-TCP [^{3}H]-ethidium [^{14}C]-amobarbital [^{125}I]-TID	60–63

Table 7.2 (continued)

Channel	Type /Current	Radioligand	Ref.
glutamate	NMDA	[^{3}H]-MK801	64
	AMPA	[^{3}H]-AMPA [^{3}H]-LY395153 [^{3}H]-Ro48–8587	65–67
	Kainate	[^{3}H]-kainic acid [^{3}H]-NBQX	68, 69
		[^{3}H]-L-glutamate [^{3}H]-CPP	70, 71
$GABA_A$		[^{3}H]-BIDN [^{3}H]-muscimol [^{3}H]-SR 95531 [^{3}H]-flunitrazepam [^{3}H]-zolpidem [^{3}H]-Ro151788(flumazenil) [^{3}H]-TBPS [^{3}H]-Ro15–4513 [^{3}H]-indiplon	72, 73
5HT3		[^{3}H]-zacopride [^{3}H]-BRL 43694 [^{3}H]-GR65630 [^{3}H]-LY278584	74
glycine		[^{3}H]-strychnine	75

Although many fluorescent-labeled ligands for ion channels, in particular peptide ligands, are commercially available or could easily be synthesized, to date ligand binding assays for screening purposes have largely been limited to using radiolabels due to the often reduced affinity of fluorescent-labeled ligands.

7.3.1 Heterogeneous Binding Assays Employing Radioligands

Since ion channels are integral membrane proteins, a suitable ion channel containing membrane preparation has to be obtained. Nowadays, recombinant cell lines expressing the ion channel under study are often employed due to the high ion channel densities that can be achieved. After incubating the membrane preparation with a high affinity radioligand ($\leq$ nM), which should exhibit a high specific radioactivity (≥ 30 Ci mmol^{-1}), until equilibrium has been reached (typically minutes to hours), channel-bound radioligand is quickly separated from free radioligand, usually by filtration and washing. For screening assays typically glass

fiber filter-mounted 96- or 384-well plates are utilized which retain ion channel-bound radioactivity on the filter. Subsequently, filter-bound radioactivity is measured using scintillation or γ-counting, depending on the isotope used. If compounds are screened in displacement experiments they are usually added to the channel preparation during the incubation phase. Plotting bound radioactivity (e.g. bound cpm) against the concentration of displacing compound allows easy calculation of an IC_{50} value for this compound as measure of its affinity for the channel. The GraphPad Prism software (GraphPad Software Inc., San Diego) which was developed for analysis of radioligand binding is most useful for data analysis and visualization.

The bee venom peptide toxin apamin is a high affinity ligand of small conductance calcium-activated potassium (SK) channels which are expressed in the cortex of rat brain [19]. The following protocol which was successfully applied for the characterization of SK channels can also serve as the basis for the configuration of other ligand binding assays with a filtration step for removing free ligand. All steps of tissue preparation were performed at 4 °C unless otherwise indicated. Cerebral cortex from rats was homogenized in 10 volumes of ice cold buffer solution [0.32 M sucrose, 5.4 mM KCl and 25 mM HEPES pH 7.0 supplemented with a protease inhibitor cocktail (Complete™, Roche)] using a glass/teflon homogenizer (1000 $g\,min^{-1}$ for 12 cycles). The homogenate was centrifuged at 1000*g* for 10 min and the supernatant re-centrifuged at 48 000*g* for 20 min. The resultant pellet was washed twice with the above solution without sucrose. The final pellet was re-suspended in this buffer and the membrane suspension divided in aliquots and stored frozen at –80 °C until further use. [^{125}I]-Apamin binding experiments were performed in 20 mM HEPES, 5.4 mM KCl, 0.2% BSA (pH 7.4) using 200 pM radioligand (specific activity 81.4 TBq $mmol^{-1}$) and 70 µg protein equivalent of rat cortex membrane preparations in a total volume of 500 µl per test tube. Nonspecific binding was determined in the presence of an excess of 1 µM unlabeled apamin. For displacement experiments the respective concentrations of compounds to be tested were added to the test tubes. After incubation for 60 min at 4 °C unbound radioligand was removed by rapid filtration through glass fiber filters (Whatman GF/C filters, pre-soaked in 0.3% polyethyleneimine for 1 h) utilizing a cell harvester (Brandel) followed by three wash steps with ice-cold buffer. Filters were placed in scintillation vials with 3.5 ml scintillation cocktail (Filter Count™, Packard) and bound radioactivity was measured using a β-counter (Packard).

7.3.2 Homogeneous Binding Assays Employing Radioligands

In order to avoid the separation of bound from free radioligand and associated necessary wash steps, a homogeneous assay format was developed which is more compatible with the requirements of HTS, largely due to reduced complexity of the experimental protocol ('mix & measure'). This scintillation proximity assay (SPA) format [31] is based on solid microspheres ('beads') containing scintillant

which are chemically modified at their surfaces to enable the coupling of molecules (Fig. 7.7). A commonly used bead type for applications with receptors and ion channels contains the lectin wheat germ agglutinin (WGA) at the surface which immobilizes membrane preparations by binding to glycosyl residues [32]. If a specific radioligand is added, it will bind to the ion channel contained in the immobilized membrane fraction and hence its emitted radiation will be in close enough proximity to activate the scintillant. The resulting emission of light around 400 nm (Fig. 7.7) can be measured with a scintillation counter. The energy released from unbound free radioligand is absorbed by the aqueous environment before it reaches the bead and hence does not activate the scintillant (Fig. 7.7). Since β-particles emitted by ^{3}H and Auger electrons released from ^{125}I have very short pathlengths in aqueous environments (<1 μm and about 17 μm), radioligands labeled with these isotopes are best suited for these assays. Due to their homogeneous format such assays can easily be automated and adapted to 384-well and higher density microplate formats which makes it especially useful for HTS. One disadvantage of 'homogeneity' is assay interference of test compounds due to quenching, which leads to reduced scintillation counting efficiency and hence reduced assay signals. In particular, yellow colored compounds will lead to quenching of the blue light emitted from the beads. A 'second generation' type of beads (SPA Imaging Beads, GE Healthcare) which contain a different scintillant that produces a red-shifted signal has been developed in order to avoid such quenching problems.

The protocol described below was routinely employed for the characterization of SK channels (Fig. 7.8) and serves as a basis for the development of other SPAs. Cell membranes were prepared from recombinant HEK293 cells stably expressing SK3 channels [18] by detaching cells cultured in 175 cm^2 T-flasks by PBS/EDTA treatment, homogenization with a Polytron at full speed for 3 bursts of 10 s in 25 mM HEPES, pH 7.4 supplemented with 5.4 mM KCl (SPA buffer) and centrifugation for 30 min at 48 000 *g*. Membrane pellets were re-suspended in SPA buffer (1–2 ml per 175 cm^2 T-flask) and membrane suspensions stored as aliquots at

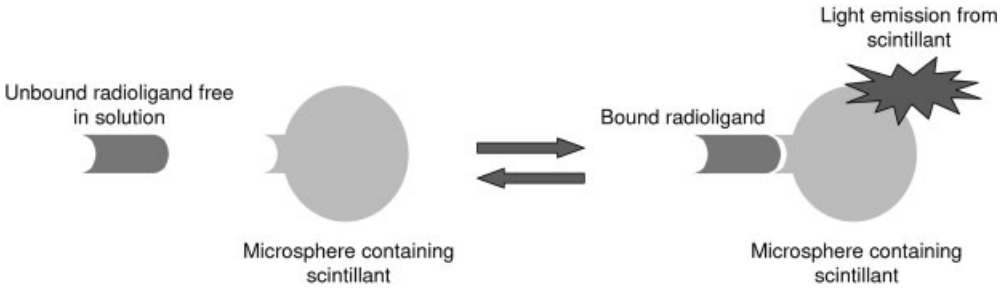

Fig. 7.7 Schematic diagram of SPA technology. Left: Binding of radioligand to an ion channel immobilized at the bead surface leads to light emission via the scintillant incorporated in the beads. Right: Free radioligand is not in close enough proximity to the beads and hence does not stimulate light emission.

–80 °C until further use. Binding experiments were carried out in 96-well microplates in a final volume of 200 µl using 10 pM [^{125}I]-apamin and 15 µg per well of SK3 channel containing membrane preparation. Each well also contains 1 mg of WGA-coated SPA beads (GE Healthcare). Nonspecific binding was determined in the presence of 1 µM unlabeled apamin. For displacement experiments the respective concentrations of compounds to be tested were added to the wells. After 15 min of incubation at room temperature with gentle shaking, the microplates were left to stand over night. Subsequently, bound radioactivity was measured with a β-counter (TopCount, Packard).

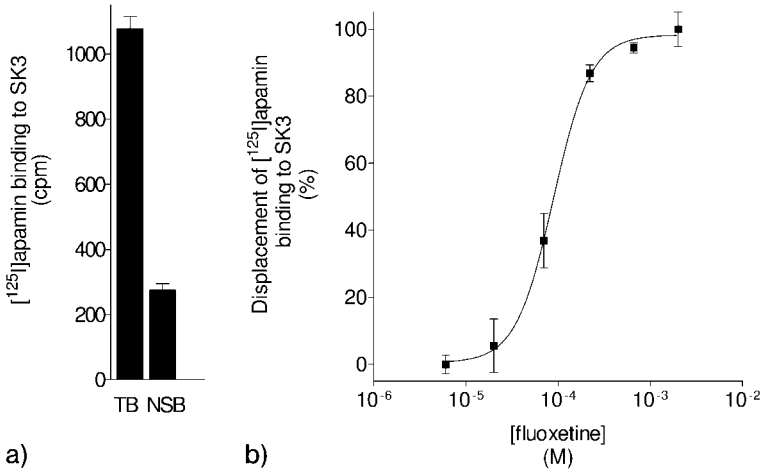

Fig. 7.8 [^{125}I]-apamin binding to membranes prepared from recombinant HEK293 cells expressing SK3 channels analyzed employing an SPA format. (A) total binding (TB) and nonspecific binding (NSB) measured in the presence of 1 µM unlabeled apamin, (B) the concentration-dependent displacement of [^{125}I]-apamin binding to SK3 channels by the antidepressant drug fluoxetine.

7.3.3
Homogeneous Binding Assays Employing Fluorescent-Labeled Ligands and Fluorescence Polarization

Since bound and free ligands show differences in molecular rotation, binding assays employing fluorescent-labeled ligands can be configured using fluorescence polarization. This read-out system is a well established analytical technique in the field of diagnostics [33]. The principle of this method is based on the observation that excitation of a fluorophore with polarized light leads to the emission of light, which will retain the initial degree of polarization depending on the rotation that occurred during the fluorescence lifetime, typically on the nanosecond time scale

[34]. At constant temperature and viscosity, the rotational relaxation time of a molecule is directly proportional to its molecular volume. Hence, if a fluorescent-labeled ligand binds to a macromolecular receptor the increase in molecular volume and concomitant decrease in rotation result in an increase in fluorescence polarization which can be measured. Advances in appropriate instrumentation over the last ten years have enabled the configuration of assays employing 96- and 384-well microplate formats. A fluorescence polarization reader can be imagined as a standard filter fluorometer with the addition of polarizing filters for the generation and detection of polarized fluorescence light. Samples are excited with polarized light and the emitted light is passed through both horizontal and vertical polarizing filters, prior to detection with a photomultiplier. Hence, the degree of polarization of the emitted light is determined in form of a ratiometric measurement, thus eliminating interferences such as 'inner filter effects'. Although dimensionless numbers are the result of such measurements, the unit P (polarization unit) was introduced for convenience and fluorescence polarization readers usually present numbers as milli P (mP).

Since fluorescence polarization is a homogeneous 'mix and measure' technology, it can easily be automated. For screening purposes assays are usually carried out in the form of competition (displacement) binding experiments (see above), determining the decrease in fluorescence polarization as a function of the concentration of competing compounds to be identified. Although significant improvements in the sensitivity of instrumentation have been achieved, high expression levels of receptors (≥ 1 pmol (mg protein)$^{-1}$) and high ligand binding affinities ($K_d \leq 10$ nM) are still necessary in order to configure robust fluorescence polarization assays. To date binding assays employing fluorescence polarization have not been widely used for the analysis of ion channels [35]. The main reason for this is that fluorescent labels such as fluorescein, Bodypy®, Texas Red™, Oregon Green® and Rhodamine Red™ are quite bulky chemical entities whose attachment to ligands often results in steric hindrance and concomitant reduction of binding affinity [36]. Moreover, coupling chemistry of such fluorescent labels for peptide ligands is quite advanced whereas considerable efforts might be necessary to create fluorescent derivatives of small organic molecules. In addition, since a substantial fraction of the fluorescent ligand needs to be bound in order to configure a robust fluorescence polarization assay, this might lead to significant ligand depletion and thus affect measured absolute IC_{50} values [35].

7.3.4 Conclusions

For primary drug screening purposes aimed at identifying novel active chemical molecules, ligand binding assays have largely been abandoned in favor of functional cell-based assays (see above and Chapters 6 and 8). The main reason for this is the limited information content of such assays which allows no distinction between agonists and antagonists. Moreover, compounds identified in binding assays will typically reflect the mode of action of the ligand used. Thus, compounds

with novel mechanisms of channel modulation cannot be readily identified. A more technical limitation relates to the fact that for many ion channels there are no selective high-affinity ligands.

Nowadays, ligand binding assays are more often employed as secondary assays in screening cascades in order to compare the molecular pharmacology of new compounds with known ligands of the channel. Furthermore, the mode of action of new compounds can be investigated if they can be labeled and used as ligands in binding assays themselves. This might also support the molecular and structural characterization of the ion channel under study since new active binding sites might be identified. The latter aspects may become increasingly important as more ion channel structures and novel modulators are discovered, and guarantee that ligand binding assays will remain an important tool for ion channel analysis.

Acknowledgements

The author would like to thank Dr. Renza Roncarati (Sienabiotech S.p.A., Discovery Research) for assistance in generating Table 7.2 and helpful discussions during the preparation of the manuscript.

References

1 J. C. Venter et al., The sequence of the human genome, *Science* **2001**, *291*, 1304–1351.

2 G. C. Terstappen, Ion channel screening technologies today, *Drug Discovery Today: Technologies* **2005**, *2*, 133–140.

3 C. Virginio, A. Giacometti, L. Aldegheri, J. M. Rimland, G. C. Terstappen, Pharmacological properties of rat alpha7 nicotinic receptors expressed in native and recombinant cell systems, *Eur. J. Pharmacol.* **2002**, *445*, 153–161.

4 M. Willow, E. A. Kuenzel, Catterall, Inhibition of voltage-sensitive sodium channels in neuroblastoma cells and synaptosomes by the anticonvulsant drugs diphenylhydantoin and carbamazepine, *Mol. Pharm.* **1984**, *25*, 228–234.

5 C. A. Rasmussen, J. L. Sutko, W. H. Barry. Effects of ryanodine and caffeine on contractility, membrane voltage, and calcium exchange in cultured heart cells, *Circ Res.* **1987**, *60*, 495–504.

6 K. G. Thampy, E. M. Barnes Jr., Gamma-aminobutyric acid-gated chloride channels in cultured cerebral neurons, *J. Biol. Chem.* **1984**, *259*, 1753–1757.

7 S. W. Weir, A. H. Weston, The effects of BRL 34915 and nicorandil on electrical and mechanical activity and on ^{86}Rb efflux in rat blood vessels, *Brit. J. Pharmacol.* **1986**, *88*, 121–128.

8 J. Denyer, J. Worley, B. Cox, G. Allenby, M Banks, HTS approaches to voltage-gated ion channel drug discovery, *Drug Discovery Today* **1998**, *3*, 323–332.

9 A. Cushing, M. J. Price-Jones, R. Graves, A. J. Harris, K. T. Hughes, D. Bleakman, D. Lodge, Measurement of calcium flux through ionotropic glutamate receptors using Cytostar-T scintillating microplates, *J. Neurosci. Methods* **1999**, *90*, 33–36.

10 J. W. Ford, E. B. Stevens, J. M. Treherne, J. Packer, M. Bushfield, Potassium channels: gene family, therapeutic relevance, high-throughput

screening technologies and drug discovery, *Prog. Drug Res.* **2002**, *58*, 133–68.
11 G. C. Terstappen, Functional analysis of native and recombinant ion channels using a high-capacity nonradioactive rubidium efflux assay, *Anal. Biochem.* **1999**, *272*, 149–155.
12 B. Hille, *Ionic Channels of Excitable Membranes*, Sinauer Associates, Sunderland, MA, **1992**
13 J-H. Zhang, T. D. Y. Chung, K. R. Oldenburg, A simple statistical parameter for use in evaluation and validation of high throughput screening assays, *J. Biomol. Screen.* **1999**, *4*, 67–73.
14 M. Garcia-Calvo, H-G. Knaus, O. B. McManus, K. M. Giangiacomo, G. Kaczorowski, M. L. Garcia, Purification and reconstitution of the high-conductance, calcium-activated potassium channel from tracheal smooth muscle, *J. Biol. Chem.* **1994**, *269*, 676–682.
15 V. K. Gribkoff, et al., Effects of channel modulators on cloned large-conductance calcium-activated potassium channels, *Mol. Pharmacol.* **1996**, *50*, 206–217.
16 A. S. Parihar, D. R. Groebe,V. E. Scott, J. Feng, X-F. Zhang, U. Warrior, M. Gopalakrishnan, C-C. Shieh, Functional analysis of large conductance Ca^{2+} activated K^+ channels: ion flux studies by atomic absorption spectrometry, *Assay Drug Dev. Technol.* **2003**, *1*, 647–654.
17 M. Kohler, B. Hirschberg, C. T. Bond, J. M. Kinzie, N. V. Marrion., J. Maylie, J. P. Adelman, Small-conductance Ca^{2+} activated K^+ channels from mammalian brain, *Science* **1996**, *273*, 1709–1714.
18 X. M. Xia, et al., Mechanism of Ca^{2+} gating in small conductance Ca^{2+}-activated K^+ channels, *Nature* **1998**, *395*, 503–507.
19 G. C. Terstappen, A. Pellacani, L. Aldegheri, F. Graziani, C. Carignani, G. Pula, C. Virginio, The antidepressant fluoxetine blocks the human small conductance calcium-activated potassium channels SK1, SK2 and SK3, *Neuroscience Lett.* **2003**, *346*, 85–88.
20 C. W. Scott, D. E. Wilkins, S. Trivedi, D. J. Crankshaw, A medium-throughput functional assay of KCNQ2 potassium channels using rubidium efflux and atomic absorption spectroscopy, *Anal. Biochem.* **2003**, *319*, 251–257.
21 K. Wang, et al.,Validation of an atomic absorption rubidium ion efflux assay for KCNQ/M- channels using the Ion Channel Reader 8000, *Assay Drug Dev. Technol.* **2004**, *2*, 525–534.
22 J. I. Vandenberg, B. W. Walker, T. J. Campbell, HERK K^+ channels: friend and foe. *Trends Pharmacol. Sci.* **2001**, *22*, 240–246.
23 W. Tang, J. Kang, X. Wu, D. Rampe, L. Wang, H. Shen, Z. Li, D. Dunnington, T. Garyantes, Development and evaluation of high throughput functional assay methods for hERG potassium channel, *J. Biomol. Screen.* **2001**, *6*, 325–331.
24 L. Stankovich, D. Wicks, S. Despotovski, D. Liang, Atomic absorption spectroscopy in ion channel screening, *Assay Drug Dev. Technol.* **2004**, *2*, 569–574.
25 G. C. Terstappen, Nonradioactive Rb^+ efflux assay and its applications in drug discovery and development, *Assay Drug Dev. Technol.* **2004**, *2*, 553–559.
26 W. A. Catterall,V. Trainer, D. G. Baden, Molecular properties of the sodium channel: a receptor for multiple neurotoxins, *Bull. Soc. Path. Exp.* **1992**, *85*, 481–485.
27 J. L. Challinor-Rogers, D. C. Kong, M. N. Iskander, G. A. McPherson, Structure-activity relationship of glibenclamide analogs: A comparison of potency as levcromakalim antagonists in rat aorta vs. affinity for [^{3}H]-glibenclamide binding to membranes from rat cerebral cortex, *J. Pharmacol. Exp. Ther.* **1995**, *273*, 778–86.
28 K. Finlayson, L. Turnbull, C. T. January, J. Sharkey, J. S. Kelly, [^{3}H]-Dofetilide binding to HERK in transfected membranes: A potential high throughput preclinical screen, *Eur. J. Pharmacol.* **2001**, *430*, 147–148.

29 D. B. Bylund, M. L. Toews, Radioligand binding methods: practical guide and tips, *Am. J. Physiol.* **1993**, *265*, L421–429.

30 R. Cheng, G. Prusoff, Relationship between the inhibition constant (K_i) and the concentration of inhibitor which causes 50 per cent inhibition (I_{50}) of an enzymatic reaction, *Biochem. Pharmacol.* **1973**, *22*, 3099–4006.

31 N. D. Cook, Scintillation proximity assay: a versatile high-throughput screening technology, *Drug Discovery Today* **1996**, *1*, 287–294.

32 F. Graziani, A. Aldegheri, G. C. Terstappen, High throughput scintillation proximity assay for the identification of FKBP-12 ligands, *J. Biomol. Screen.* **1999**, *4*, 3–7.

33 W. B. Dandliker, V. A. de Saussure, Fluorescence polarization in immunochemistry, *Immunochemistry* **1970**, *7*, 799–828.

34 P. Perrin, Polarisation de la lumière de fluorescence, *J. Phys. Radium* **1926**, *7*, 390–401.

35 M. Allen, J. Reeves, G. Mellor, High throughput fluorescence polarization: a homogeneous alternative to radioligand binding for cell surface receptors, *J. Biomol. Screen.* **2000**, *5*, 63–69.

36 P. Wu, M. Brasseur, W. Schindler, A high throughput STAT binding assay using fluorescence polarization, *Anal. Biochem.* **1997**, *249*, 29–36.

37 H. Glossmann, J. Striessnig, Molecular properties of calcium channels, *Rev. Physiol. Biochem. Pharmacol.* **1990**, *114*, 1–105.

38 A. Koschak, D. Reimer, I. Huber, M. Grabner, H. Glossmann, J. Engel, J. Striessnig, $Ca_v1.3$ subunits can form L-type calcium channels activating at negative voltages, *J. Biol. Chem.* **2001**, *276*, 22100–22106.

39 M. Hagiwara, S. Adachi-Akahne, T. Nagao, High-affinity binding of [^{3}H]-DTZ323 to the diltiazem-binding site of L-type Ca^{2+} channels, *Eur. J. Pharmacol.* **2003**, *466*, 63–71.

40 M. E. Williams, et al., Structure and functional expression of an ω-conotoxin-sensitive human N-type calcium channel, *Science* **1992**, *257*, 389–395.

41 P. Favreau, et al., A new omega-conotoxin that targets N-type voltage-sensitive calcium channels with unusual specificity, *Biochemistry* **2001**, *40*, 14567–14575.

42 R. J. Lewis, et al., Novel omega-conotoxins from Conus catus discriminate among neuronal calcium channel subtypes, *J. Biol. Chem.* **2000**, *275*, 35335–35344.

43 J. W. West, T. Scheuer, L. Maechler, W. A. Catterall, Efficient expression of rat brain type IIA Na^+ channel subunits in a somatic cell line, *Neuron* **1992**, *8*, 59–70.

44 J. C. Rogers, Y. Qu, T. N. Tanada, T. Scheuer, W. A. Catterall, Molecular determinants of high affinity binding of ù-scorpion toxin and sea anemone toxin in the S3-S4 extracellular loop in domain IV of the Na^+ channel subunit, *J. Biol. Chem.* **1996**, *271*, 15950–15962.

45 S. Cestèle, Y. Qu, J. C. Rogers, H. Rochat, T. Scheuer, W. A. Catterall, Voltage sensor-trapping: enhanced activation of sodium channels by ω-scorpion toxin bound to the S3-S4 loop in domain II, *Neuron* **1998**, *21*, 919–931.

46 R. S. Sheldon, N. J. Cannon, H. J. Duff, Binding of [^{3}H]-batrachotoxinin A benzoate to specific sites on rat cardiac sodium channels, *Mol. Pharmacol.* **1986**, *30*, 617–623.

47 M. Taouis, R. S. Sheldon, R. J. Hill, H. J. Duff, Cyclic AMP-dependent regulation of the number of [^{3}H]-batrachotoxinin benzoate binding sites on rat cardiac myocytes, *J. Biol. Chem.* **1991**, *266*, 10300–10304.

48 A. J. Bourdelais, S. Campbell, H. Jacocks, J. Naar, J. L. Wright, J. Carsi, D. G. Baden, Brevenal is a natural inhibitor of brevetoxin action in sodium channel receptor binding assays, *Cell. Mol. Neurobiol.* **2004**, *24*, 553–63.

49 M. Yotsu-Yamashita, K. Nishimori, Y. Nitanai, M. Isemura, A. Sugimoto, T. Yasumoto, Binding properties of [^{3}H]-PbTx-3 and [^{3}H]-saxitoxin to brain membranes and to skeletal muscle

membranes of puffer fish Fugu pardalis and the primary structure of a voltage-gated Na^+ channel alpha-subunit (fMNa1) from skeletal muscle of F. pardalis, *Biochem. Biophys. Res. Commun.*, **2000**, *267*, 403–412.

50 O. Shamotienko, S. Akhtar, C. Sidera, F. A. Meunier, B. Ink, M. Weir, J. O. Dolly, Recreation of neuronal K_v1 channel oligomers by expression in mammalian cells using Semliki Forest virus, *Biochemistry* **1999**, *38*, 16766–16776.

51 J. Racape, A. Lecoq, R. Romi-Lebrun, J. Liu, M. Kohler, M. L. Garcia, A. Menez, S. Gasparini, Characterization of a novel radiolabeled peptide selective for a subpopulation of voltage-gated potassium channels in mammalian brain, *J. Biol. Chem.* **2002**, *277*, 3886–3893.

52 P. J. Chiu, et al., Validation of a [^{3}H]-astemizole binding assay in HEK293 cells expressing HERG K^+ channels, *J. Pharmacol. Sci.* **2004**, *95*, 311–319.

53 K. Finlayson, A. J. Pennington, J. S. Kelly, [^{3}H]-dofetilide binding in SHSY5Y and HEK293 cells expressing a HERG-like K^+ channel, *Eur. J. Pharmacol.* **2001**, *412*, 203–212.

54 R. Davis-Taber, et al., [^{125}I]A-312110, a novel high-affinity 1,4-dihydropyridine ATP-sensitive K^+ channel opener: characterization and pharmacology of binding, *Mol. Pharmacol.* **2003**, *64*, 143–153.

55 P. W. Manley, C. Loffler-Walz, U. Russ, A. Hambrock, T. Moenius, U. Quast, Synthesis and characterization of a novel tritiated K_{ATP} channel opener with a benzopyran structure, *Br. J. Pharmacol.* **2001**, *133*, 275–85.

56 M. Hanner, R. Vianna-Jorge, A. Kamassah., W. A. Schmalhofer, H. G. Knaus, G. J. Kaczorowski, M. L. Garcia, The beta subunit of the high conductance calcium-activated potassium channel. Identification of residues involved in charybdotoxin binding, *J. Biol. Chem.* **1998**, *273*, 16289–16296.

57 A. Koschak, R. O. Koch, J. Liu, G. J. Kaczorowski, P. H. Reinhart, M. L. Garcia, H. G. Knaus, [^{125}I]-Iberiotoxin-D19Y/Y36F, the first selective, high specific activity radioligand for high-conductance calcium-activated potassium channels, *Biochemistry* **1997**, *36*, 1943–1952.

58 D. O. Kiesewetter, E. M. Jagoda, J. E. Starrett Jr, V. K. Gribkoff, P. Hewawasam, N. Srinivas, D. Salazar, W. C. Eckelman, Radiochemical synthesis and biodistribution of a novel maxi-K potassium channel opener, *Nucl. Med. Biol.* **2002**, *29*, 55–59.

59 M. Hugues, D. Duval, P. Kitabgi, M. Lazdunski, J. P. Vincent, Preparation of a pure monoiodo derivative of the bee venom neurotoxin apamin and its binding properties to rat brain synaptosomes, *J. Biol. Chem.* **1982**, *257*, 2762–2769.

60 D. J. Anderson, S.P Arneric, Nicotinic receptor binding of [^{3}H]cytisine, [^{3}H]-nicotine and [^{3}H]-methylcarbamylcholine in rat brain, *Eur. J. Pharmacol.* **1994**, *253*, 261–267.

61 D. Gnadisch, E. D. London, P. Terry, G. R. Hill, A. G. Mukhin, High affinity binding of [^{3}H]-epibatidine to rat brain membranes, *Neuroreport* **1999**, *10*, 1631–1636.

62 H. A. Navarro, D. Zhong, P. Abraham, H. Xu, F. I. Carroll, Synthesis and pharmacological characterization of [^{125}I]-iodomethyllycaconitine ([^{125}I]-iodo-MLA). A new ligand for the alpha 7 nicotinic acetylcholine receptor, *J. Med. Chem.* **2000**, *43*, 142–145.

63 H. R. Arias, J. R. Trudell, E. Z. Bayer, B. Hester, E. A. McCardy, M. P. Blanton, Noncompetitive antagonist binding sites in the torpedo nicotinic acetylcholine receptor ion channel. Structure-activity relationship studies using adamantane derivatives, *Biochemistry* **2003**, *42*, 7358–7370.

64 F. Murray, J. Kennedy, P. H. Hutson, J. Elliot, I. Huscroft, K. Mohnen, M. G. Russell, S. Grimwood, Modulation of [^{3}H]-MK-801 binding to NMDA receptors in vivo and in vitro, *Eur. J. Pharmacol.* **2000**, *397*, 263–270.

65 L. Bunch, T. H. Johansen, H. Braunner-Osborne, T. B. Stensbol, T. N. Johansen, P. Krogsgaard-Larsen, U. Madsen, Synthesis and receptor

binding affinity of new selective GluR5 ligands, *Bioorg. Med. Chem.* **2001**, *9*, 875–879.

66 A. M. Linden, H. Yu, H. Zarrinmayeh, W. J. Wheeler, P. Skolnick, Binding of an AMPA receptor potentiator ([^{3}H]-LY395153) to native and recombinant AMPA receptors, *Neuropharmacology* **2001**, *40*, 1010–1018.

67 V. Mutel, et al., Binding characteristics of a potent AMPA receptor antagonist [^{3}H]Ro 48–8587 in rat brain, *J. Neurochem.* **1998**, *71*, 418–426.

68 N. Crawford, T. K. Lang, D. S. Kerr, D. J. de Vries, High-affinity [^{3}H] kainic acid binding to brain membranes: a reevaluation of ligand potency and selectivity, *J. Pharmacol. Toxicol. Methods* **1999**, *42*, 121–125.

69 K. K. Dev, V. Petersen, T. Honore, J. M. Henley, Pharmacology and regional distribution of the binding of 6-[^{3}H]-nitro-7-sulphamoylbenzo[f]-quinoxaline-2,3-dione to rat brain, *J. Neurochem.* **1996**, *67*, 2609–2612.

70 L. H. Martini, C. R. Souza, P. B. Marques, J. B. Calixto, R. A. Yunes, D. O. Souza, Compounds extracted from Phyllantus and Jatropha elliptica inhibit the binding of [^{3}H]-glutamate and [^{3}H]-GMP-PNP in rat cerebral cortex membrane, *Neurochem. Res.* **2000**, *25*, 211–215.

71 R. H. Porter, R. S. Briggs, P. J. Roberts, Modulation of [^{3}H]3-((+-)-2-carboxypiperazin-4-yl)propyl-1-phosphonic acid ([^{3}H]CPP) binding by ligands acting at the glycine and the polyamine sites of the rat brain NMDA receptor complex, *Eur. J. Pharmacol.* **1992**, *227*, 83–88.

72 J. J. Rauh, et al., Effects of [^{3}H]-BIDN, a novel bicyclic dinitrile radioligand for GABA-gated chloride channels of insects and vertebrates, *Br. J. Pharmacol.* **1997**, *121*, 1496–1505.

73 S. K. Sullivan, R. E. Petroski, G. Verge, R. S. Gross, A. C. Foster, D. E. Grigoriadis, Characterization of the interaction of indiplon, a novel pyrazolopyrimidine sedative-hypnotic, with the GABAA receptor, *J. Pharmacol. Exp. Ther.* **2004**, *311*, 537–546.

74 S. C. Lummis, J. Baker, Radioligand binding and photoaffinity labelling studies show a direct interaction of phenothiazines at 5-HT3 receptors, *Neuropharmacology* **1997**, *36*, 665–70.

75 R. J. Vandenberg, C. R. French, P. H. Barry, J. Shine, P. R. Schofield, Antagonism of ligand-gated ion channel receptors: two domains of the glycine receptor alpha subunit form the strychnine-binding site, *Proc. Natl. Acad. Sci. U S A.* **1992**, *89*, 1765–1769.